Molecular Neurobiology (2024) 61:4691–4704
https://doi.org/10.1007/s12035-023-03865-z

Light-Driven Sodium Pump as a Potential Tool for the Control of Seizures in Epilepsy

Alina M. Trofimova[1] · Dmitry V. Amakhin[1] · Tatyana Y. Postnikova[1] · Vasilii S. Tiselko[1] · Alexey Alekseev[2,3] · Elizaveta Podoliak[2,4] · Valentin I. Gordeliy[2,5] · Anton V. Chizhov[1,6] · Aleksey V. Zaitsev[1]

Received: 12 August 2023 / Accepted: 6 December 2023 / Published online: 20 December 2023

Abstract

The marine flavobacterium Krokinobactereikastus light-driven sodium pump (KR2) generates an outward sodium ion current under 530 nm light stimulation, representing a promising optogenetic tool for seizure control. However, the specifics of KR2 application to suppress epileptic activity have not yet been addressed. In the present study, we investigated the possibility of KR2 photostimulation to suppress epileptiform activity in mouse brain slices using the 4-aminopyridine (4-AP) model. We injected the adeno-associated viral vector (AAV-PHP.eB-hSyn-KR2-YFP) containing the KR2 sodium pump gene enhanced with appropriate trafficking tags. KR2 expression was observed in the lateral entorhinal cortex and CA1 hippocampus. Using whole-cell patch clamp in mouse brain slices, we show that KR2, when stimulated with LED light, induces a substantial hyperpolarization of entorhinal neurons. However, continuous photostimulation of KR2 does not interrupt ictal discharges in mouse entorhinal cortex slices induced by a solution containing 4-AP. KR2-induced hyperpolarization strongly activates neuronal HCN channels. Consequently, turning off photostimulation resulted in HCN channel-mediated rebound depolarization accompanied by a transient increase in spontaneous network activity. Using low-frequency pulsed photostimulation, we induced the generation of short HCN channel-mediated discharges that occurred in response to the light stimulus being turned off; these discharges reliably interrupt ictal activity. Thus, low-frequency pulsed photostimulation of KR2 can be considered as a potential tool for controlling epileptic seizures.

Keywords KR2-pump · Epilepsy · Low frequency stimulation · Optogenetic silencing · Entorhinal cortex

Introduction

Up to 30% of patients with epilepsy are resistant to existing pharmacological treatments [1]. In addition, side effects of existing antiepileptic drugs include cognitive impairment, depression, and anxiety [2, 3]. This calls for the development of alternative approaches to the treatment of epilepsy. One such potential alternative is optogenetic stimulation, in which light-driven membrane proteins (opsins) are expressed by viral vectors in target neurons and activated by a specific wavelength of light [4–7]. The ability to control the activity of specific cell types may provide a more precise and efficient way to disrupt epileptic activity than classical pharmacological interventions [8].

The recently discovered novel microbial rhodopsin from the marine flavobacterium Krokinobactereikastus (KR2) is the first known light-driven sodium pump [9]. Several homologous members of this microbial rhodopsin class have subsequently been identified in other bacteria [10–12]. KR2

✉ Aleksey V. Zaitsev
aleksey_zaitsev@mail.ru

1 Sechenov Institute of Evolutionary Physiology and Biochemistry, Saint Petersburg, Russia

2 Research Center for Molecular Mechanisms of Aging and Age-Related Diseases, Moscow Institute of Physics and Technology (National Research University), Dolgoprudny, Russia

3 Present Address: Institute for Auditory Neuroscience and InnerEarLab, University Medical Center Göttingen, Göttingen, Germany

4 Present Address: Department of Ophthalmology, Universitäts-Augenklinik Bonn, University of Bonn, Bonn, Germany

5 Institut de Biologie Structurale (IBS), Université Grenoble Alpes, CEA, CNRS, Grenoble, France

6 MathNeuro Team, Inria Centre at Université Côte d'Azur, Sophia Antipolis, France

is of particular interest as a potential next-generation optogenetic tool because, when activated by green light (530 nm), it pumps out sodium ions, leading to a substantial hyperpolarization of neurons and a consequent decrease in their activity. For example, in a culture of rat cortical neurons, activation of the KR2 photocurrent led to a strong suppression of firing and hyperpolarization of the cell membrane [13, 14]. Exposure of transgenic *Caenorhabditis elegans* expressing KR2 to green light in vivo suppressed the locomotion of the worm [13]. Another advantage of KR2 as a potential new-generation optogenetic silencer of neuronal activity is its presumed lack of significant effect on cellular pH balance [9], which is a documented problem for other light-driven sodium opsins [15–17].

Thus, the use of a new light-driven sodium pump seems to be a very promising approach to suppress epileptic activity. However, to date, there are no studies on the effect of KR2 on epileptic activity or on the neurons in brain regions involved in its generation. Therefore, we expressed KR2 in the mouse entorhinal cortex and hippocampus, the brain regions responsible for the generation of abnormal activity in temporal epilepsy [18]. In the present study, we provide an electrophysiological description of KR2 photocurrent properties and their effects on neuronal membrane voltage in mouse brain slices. We also describe the HCN channel-mediated rebound depolarization and propose a KR2 photostimulation protocol that effectively terminates ictal-like activity in the 4-aminopyridine (4-AP) model of epileptic seizures.

Methods

Animals

Experiments were performed in the C57BL/J mouse strain ($n = 8$, aged 4–6 months, Rappolovo Animal Facility, Russia). Only male animals were used in the experiments. All animal procedures complied with the European Community Council Directive 86/609/EEC and were approved by the Animal Care and Use Committee of the Sechenov Institute of Evolutionary Physiology and Biochemistry of the Russian Academy of Sciences (Protocol № 1–7 / 2022 of the meeting № 1 of January 27, 2022).

Adeno-Associated Virus (AAV) Production

For virus production, we used the KR2 gene in a construct with an N-terminal C2C1 tag (C2C1), Kir2.1 membrane trafficking signal (TS) and ER export signal (ES). The gene (C2C1_KR2_TS_EYFP_ES) was cloned into the pAAV backbone behind the human synapsin promoter (hSyn) using BamHI and EcoRI digestion sites. The synapsin promoter is neuron specific [19, 20], allowing KR2 to be expressed exclusively in neurons. AAVs were generated by transfecting HEK-293 T cells with polyethyleneimine (25,000 MW, Polysciences, USA). The transfection involved triple transfection of HEK-293 T cells with the pHelper plasmid (TaKaRa/Clontech), a plasmid providing the viral capsid AAV-PHP.eB (Addgene plasmid #103005), and a plasmid containing the KR2 gene. After 72 h, viral particles were harvested from the medium, and after 120 h, they were harvested from both the medium and the cells. Viral particles from the medium were precipitated with 40% polyethylene glycol 8000 (Acros Organics, Germany) in 500 mM NaCl for 2 h at 4 °C. The precipitated particles were then combined with cell pellets for further processing after centrifugation at 4000 × g for 30 min. The cell pellets were resuspended in a solution of 500 mM NaCl, 40 mM Tris, 2.5 mM MgCl2 (pH 8), and 100 U/ml salt-activated nuclease (Arcticzymes, USA) and incubated at 37 °C for 30 min. The cell lysates were then clarified by centrifugation at 2000 × g for 10 min and subjected to purification using iodixanol (Optiprep, Axis Shield, Norway) step gradients (15, 25, 40, and 60%) at 320,006 × g for 2.25 h. Viruses were concentrated using Amicon filters (EMD, UFC910024) and formulated in sterile phosphate-buffered saline (PBS) supplemented with 0.001% Pluronic F-68 (Gibco, Germany). Viral stocks were stored at − 80 °C until the day of the experiment. The AAV production protocol is the same as previously described [21].

Stereotaxic Virus Injection

Mice were anesthetized with a mixture of zoletil-100 (20 mg/kg; Virbac, France) and xylazine (15 mg/kg; Interchemie, Netherlands) and placed in a stereotaxic apparatus (SM-15 Narishige, Tokyo, Japan). AAV-PHP.eB-hSyn-KR2-YFP vector was injected into the lateral entorhinal cortex (2 µL at a rate of 0.1 µL/min). Injection coordinates were as follows: − 4.5 mm anteroposterior, 4 mm mediolateral, and − 3.5 mm dorsoventral to the bregma [22]. AAV was injected into the right and left hemispheres in random order. After all surgical procedures, mice were transferred to heated cages for 24 h and then returned to their home cages. Experiments were conducted 1 month after injection.

Acute Slice Preparation

Mice were anesthetized with isoflurane (Karizoo, Spain) and decapitated, the brain was rapidly removed, and horizontal hippocampal-entorhinal brain slices (350 µm) were cut without any tilting angle with a vibratome HM 650 V (Microm, Walldorf, Germany) in ice-cold N-methyl-D-glucamine (NMDG) solution aerated with carbogen (95% O2 and 5% CO2). Composition of the NMDG solution (in mM): 110 NMDG, 2.5 KCl, 1.2 NaH_2PO_4, 10 $MgSO_4$, 0.5 $CaCl_2$, 25

$NaHCO_3$, 25 dextrose, pH was adjusted to 7.3–7.4 with 1 M HCl. After cutting, the slices were placed in artificial cerebrospinal fluid (ACSF) (in mM: 126 NaCl, 2.5 KCl, 1.25 NaH_2PO4, 1 $MgSO_4$, 2 $CaCl_2$, 24 $NaHCO_3$, 10 dextrose). Slices were incubated at 35 °C for 10 min and then at room temperature for 1 h. Microphotographs were taken at × 50 and × 400 magnification using a Leica AF 7000 fluorescence microscope (Leica Microsystems, Wetzlar, Germany).

4-AP Model of Epileptic Seizures

To facilitate the generation of ictal-like activity in the entorhinal cortex and reduce interictal activity generated by hippocampal CA3 neurons [23, 24], Schafer's collaterals were incised between hippocampal areas CA3 and CA2. The mouse brain slice was then perfused with the proepileptic solution (in mM): 125 NaCl, 3.5 KCl, 1.25 NaH_2PO_4, 0.25 $MgSO_4$, 2 $CaCl_2$, 24 $NaHCO_3$, 13 D-glucose, and 0.1 4-AP. This resulted in the stable generation of ictal-like discharges in the entorhinal cortex. The characteristics of individual ictal discharges in the comparable model have been described in detail in our previous works [25–27]. Stable ictal activity was recorded for at least 15 min prior to KR2 photostimulation.

Electrophysiological Recordings

After incubation, individual slices were placed in the experimental chamber. The recordings were performed at 30 °C in ACSF. The flow rate in the perfusion chamber was 5–6 ml/min. Both whole-cell patch-clamp and extracellular field potential recordings were performed.

For the whole-cell patch-clamp recordings, neurons from the entorhinal cortex were visualized using a Nikon Eclipse FN1 microscope (Nikon; Tokyo, Japan) equipped with differential interference contrast optics, a Grasshopper3 video camera (FLIR Systems; Wilsonville, OR, USA), an optical filter set for fluorescence imaging (the YFP MXR00107 filter cube, Semrock, West Henrietta, NY, USA), and BLS-LCS-0505–03-22 and BLS-LCS-0530–03-22 high-power LED collimator sources with 135 and 200 mW maximum output power (Mightex Systems, North York, ON, Canada). KR2 expression was observed in all types of neurons [20], but in this study we focused on researching the effects of KR2 photostimulation on excitatory cells only. Principal neurons were identified based on their triangular soma and regular firing pattern. Patch electrodes (3–4 MΩ) were made from borosilicate glass capillaries (World Precision Instruments, Sarasota, FL, USA) using a P-1000 micropipette puller (Sutter Instrument, Novato, CA, USA). The electrodes were filled with a potassium gluconate-based solution (in mM): 135 K-gluconate, 10 NaCl, 5 EGTA, 10 HEPES, 4 ATP-Mg, and 0.3 GTP. The osmolarity of the pipette solutions was adjusted to 290–300 mOsm and the pH to 7.25. Whole-cell recordings were performed with a HEKA EPC-10 amplifier (HEKA, Harvard Bioscience, Inc., Holliston, MA, USA) using PatchMaster 1.2 software (HEKA). Data were filtered at 10 kHz and sampled at 33 kHz. Access resistance was less than 20 MΩ and remained stable throughout the experiments (increase ≤ 20%) in all cells included in the analysis.

Extracellular field excitatory postsynaptic potentials (fPSPs) were recorded in the deep layers of the mouse entorhinal cortex using glass microelectrodes (0.2–1.0 MΩ) filled with ACSF. The fPSPs were amplified using a Model 1800 amplifier (A-M Systems, Carlsborg, WA, USA), digitized using an ADC/DAC NI USB-6211 (National Instruments, Austin, TX, USA), and stored on a computer using WinWCP v5 software (University of Strathclyde, Glasgow, UK). Data were bandpass filtered between 2.9 and 10 kHz and digitized at 25 kHz.

Photostimulation

KR2 was excited with light of 530 nm wavelength. Both continuous photostimulation of 0.5–10 s duration and intermittent photostimulation at the frequencies of 0.2–2 Hz were applied. The voltage-clamp mode was used to record the KR2 photocurrents in pyramidal neurons. The steady-state photocurrent was measured during the last 100 ms of a 1000 ms photostimulation. The zero-current-clamp mode was used to record the deviations in membrane voltage, induced by photostimulation. Both the whole-cell patch-clamp and fPSC recordings were used to assess the effects of photostimulation on epileptiform activity.

Analysis of Electrophysiological Recordings

Recordings were analyzed using the Clampfit 10.4 program (Axon Instruments, San Jose, CA, USA) and custom software written in Wolfram Mathematica v12 (Wolfram Research, Champaign, IL, USA). The decay time constants for each KR2 photocurrent were assessed by fitting the current decay phase (from 90% of its peak amplitude) with a double exponential function:

$$f(t) = a_1 e^{-t/\tau_1} + a_2 e^{-t/\tau_2} + c \quad (1)$$

where $\tau 1$ and $\tau 2$ are the slow and fast time constants, respectively, the $a1$ and $a2$ are the amplitudes of the slow-decaying and fast-decaying components, and c is the constant coefficient.

The weighted decay time constant (τ_w, ms) was calculated as follows:

$$\tau_w = \frac{a_1\tau_1 + a_2\tau_2}{a_1 + a_2} \quad (2)$$

Rebound potential area was calculated as the 10 s integral of the time–voltage plot following the photostimulation turn off, with the baseline membrane potential adjusted to the value observed before the photostimulation.

The membrane potential noise ratio was calculated as the ratio of the standard deviations of two membrane potential recording fragments of equal length (4–5 s), obtained before and after the photostimulation.

Registration of Extracellular Potassium Concentration

To assess changes in an extracellular potassium concentration, a potassium-selective electrode (tip filled with potassium ionophore I—cocktail A, Sigma-Aldrich, St. Louis, MO, USA, the remaining volume filled with 100 mM KCl) was placed in the extracellular space next to the patch-electrode. Changes in electrode voltage were recorded using a HEKA 10 USB patch-clamp amplifier in current-clamp mode. The extracellular potassium concentration ($[K^+_o]$) at a given time (t) was calculated from the electrode voltage ($V(t)$) as follows:

$$\left[K^+_o\right](t) = 2.5e^{SV(t)} \quad (3)$$

where $S = 0.044\ \mathrm{mV}^{-1}$ is the scaling factor, which was estimated by applying solutions with different $[K^+_o]$ at the tips of ionophore-filled electrodes using a fast application system (HSSE-2/3, ALA Scientific Instruments Inc., Farmingdale, NY, USA).

Statistical Analysis

Sigmaplot 15 (Systat Software Inc., San Jose, CA, USA) was used for statistical data analysis. Dixon's Q test (at 95% confidence level) was used to reject outliers. The normality of the sample data was assessed using the Kolmogorov–Smirnov test. As the data were not normally distributed, statistical significance was assessed using Kruskal–Wallis one-way analysis or Friedman RM analysis. Results were considered significant at $p < 0.05$. Dunn's post hoc test was used for multiple comparisons with the control group. All data are expressed as mean ± SEM; "n" refers to the number of neurons.

Drugs

The HCN channel blocker ZD7288 (25 µM) and the voltage-gated sodium channel blocker tetrodotoxin (TTX, 0.5 µM) were purchased from Alomone Labs (Jerusalem, Israel). All the other chemicals were purchased from Sigma-Aldrich.

Results

KR2 Photocurrents Induce Hyperpolarization of the Principal Neurons of the Mouse Entorhinal Cortex

The entorhinal cortex and hippocampus are responsible for the generation of ictal activity in temporal lobe epilepsy [28, 29]. To achieve KR2 expression in these areas, we injected the viral vector into the lateral entorhinal cortex. One month later, the horizontal slices were cut. Strong KR2 expression was observed in the entorhinal cortex and hippocampal CA1 field (Fig. 1A, B). We performed the whole-cell patch-clamp recordings from the pyramidal neurons of the deep lateral entorhinal cortex, which showed strong YFP fluorescence. Photostimulation of KR2-expressing pyramidal neurons produced a sharp current peak followed by a smaller steady-state current (Fig. 1C, D). We first examined the dependence of the KR2 peak and steady-state photocurrents on light radiant flux. Both currents increased with light intensity; the peak current reached its maximum amplitude when the light intensity was 3 times higher than that for the steady-state currents (156 ± 17 mW vs. 47 ± 13 mW, $n = 8$). When stimulated with a saturating light intensity, the peak-to-steady-state ratio of KR2 photocurrents was 3.0 ± 0.2 ($n = 8$), and the current decayed with a weighted time constant of 10 ± 3 ms (at − 60 mV). In all subsequent experiments, the KR2 photocurrent was induced by light of saturating intensity. Next, we examined how the KR2 photocurrent affected the membrane potential of pyramidal neurons (Fig. 1E). KR2 photostimulation induced an electrogenic hyperpolarization with a peak amplitude of 24 ± 4 mV ($n = 13$) and the steady-state amplitude of about 19 ± 3 mV ($n = 13$). We hypothesized that that such significant hyperpolarization is capable of terminating ictal-like activity. We tested this hypothesis using the 4-AP model of epileptiform activity in vitro.

Continuous KR2 Photostimulation Fails to Terminate the Ictal Discharges in the Slice

After replacing ACSF with a proepileptic solution, stable ictal activity developed in the mouse entorhinal cortex (Fig. 2A). We turned on photostimulation to hyperpolarize entorhinal cortex neurons at the time moment preceded the emergence of ictal discharges predicted from visual observations of spontaneous activity patterns. However, in the presence of prolonged photostimulation of KR2, ictal discharges still emerged in 5 out of 5 recordings (Fig. 2C). Interestingly, the amplitude of hyperpolarization induced

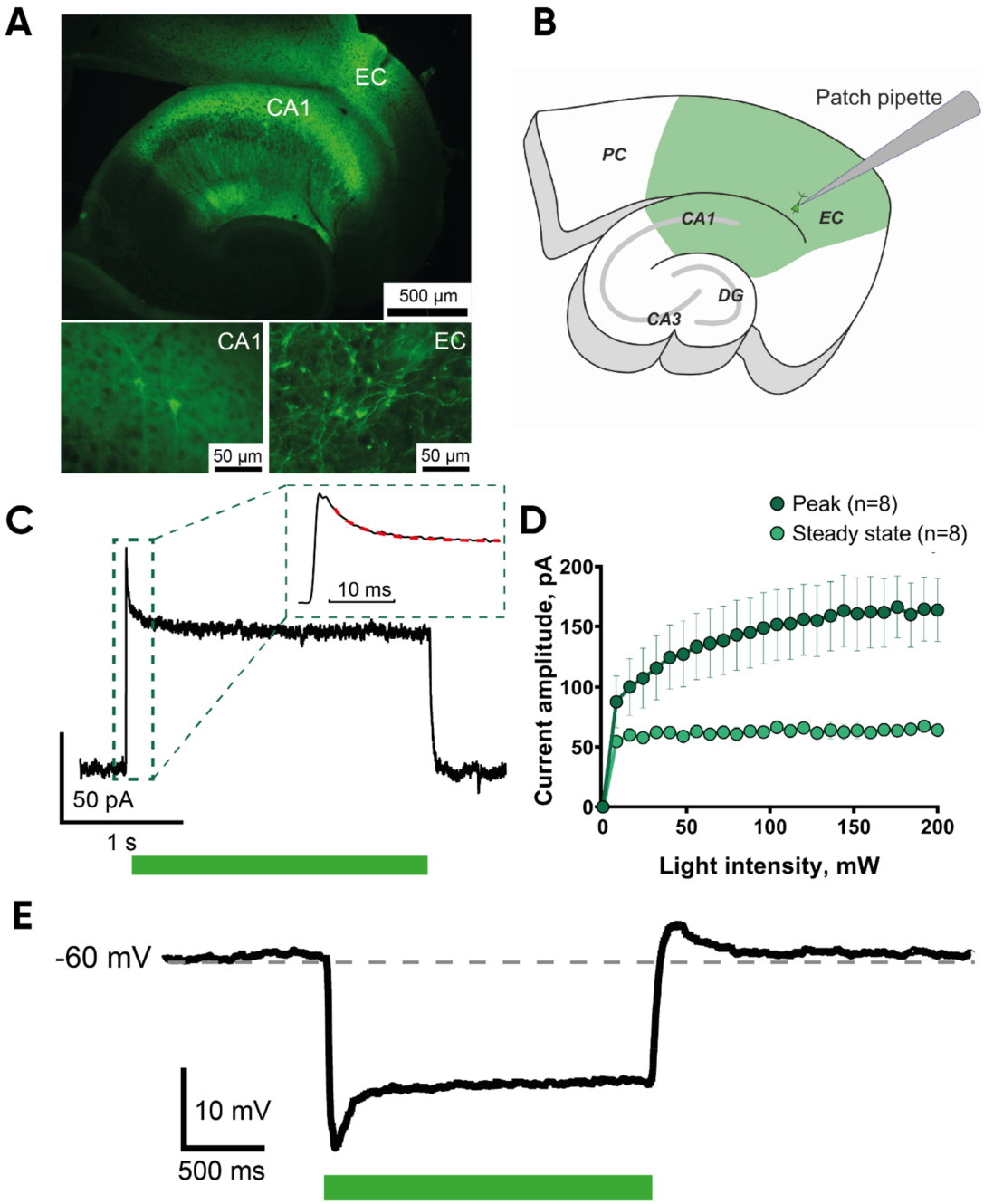

Fig. 1 The KR2 expression in the entorhinal cortex and the properties of KR2-photocurrents. **A** An example of KR2-expression in a mouse brain slice. A YFP fluorescent label marks the KR2-expressing neurons, magnifications are × 50 and × 400 accordingly. **B** The scheme shows the horizontal brain slice with the YFP fluorescence (green area) and the location of a patch electrode. EC—the entorhinal cortex, PC—perirhinal cortex, DG—dentate gyrus, CA1 and CA3—the hippocampal areas. **C** A representative recording of the photocurrent induced in the entorhinal pyramidal neuron by the photostimulation (the holding voltage was − 70 mV). The framed inset represents the extended current peak, with the decay phase being fitted with the biexponential function. **D** The dependence of the peak- and steady-state currents on the light intensity (V_{hold} = − 70 mV). **E** The representative recording of the membrane potential of the pyramidal neuron during the KR2 photostimulation

by KR2 activation at the onset of the ictal discharge did not exceed − 10 mV. This can be attributed to the GABA-mediated spontaneous activity, which is always present before the ictal discharges and should decrease the input resistance, resulting in the smaller responses to KR2 activation [30]. A significant increase of the membrane conductance was also observed during the late clonic stage of an ictal discharge [25], which might also lead to the

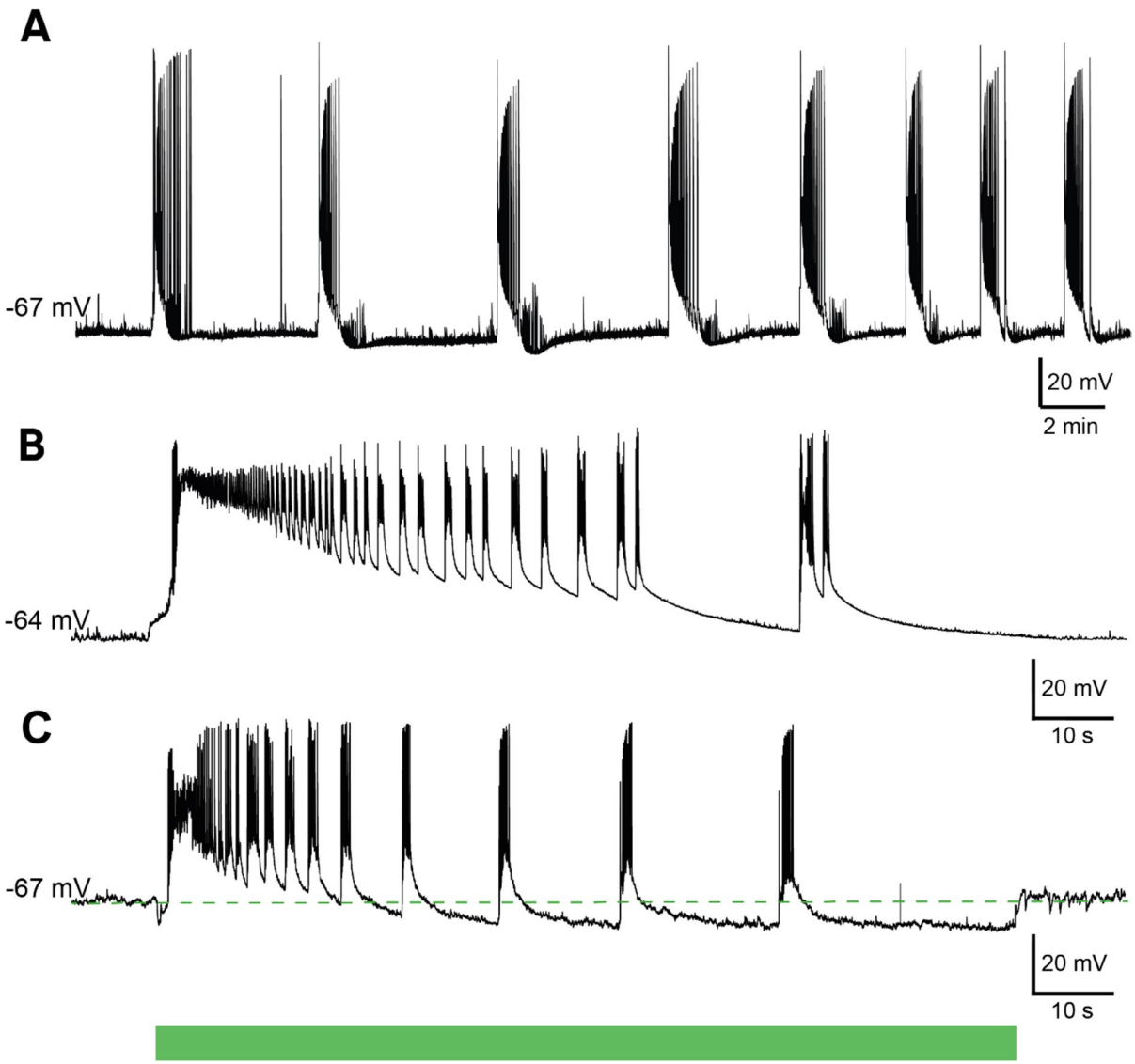

Fig. 2 The effect of KR2 photostimulation on the ictal activity in a mouse brain slice. **A** A representative recording of the membrane voltage of the entorhinal cortex pyramidal neuron during perfusion with 4-AP-containing solution. Stable generation of ictal-like discharges is observed. **B** A representative ictal-like discharge. **C** The recording from the same neuron as in **B**. Prolonged activation of the KR2 photocurrent fails to terminate the ictal-like discharge

shunting of KR2 response. This result indicates that continuous KR2 photostimulation is unable to prevent the ictal discharges in the 4-AP model.

KR2-Photocurrent-Induced Hyperpolarization Causes the Rebound Depolarization

As the continuous photostimulation failed to prevent ictal activity, we attempted to develop an alternative protocol, which utilizes the intermittent photostimulation of KR2. We have previously reported that low-frequency optogenetic stimulation of principal neurons of the mouse entorhinal cortex prevents ictal activity in the 4-AP model of epilepsy in vitro [31]. In contrast, low-frequency hyperpolarization of pyramidal neurons using archaerhodopsin photostimulation did not affect ictal activity [31]. Therefore, intermittent KR2 photic stimulation was expected to be ineffective. However, a significant rebound depolarization of pyramidal neurons was observed in response to turning off KR2 photostimulation (Fig. 3A–D). The magnitude of the rebound depolarization increased with the duration of photostimulation (Fig. 3B). We hypothesized that this transient depolarization could be used for indirect stimulation of entorhinal neurons and investigated its underlying mechanisms by assessing the contributions of hyperpolarization-activated currents, transient increase of network activity and change of ionic gradients.

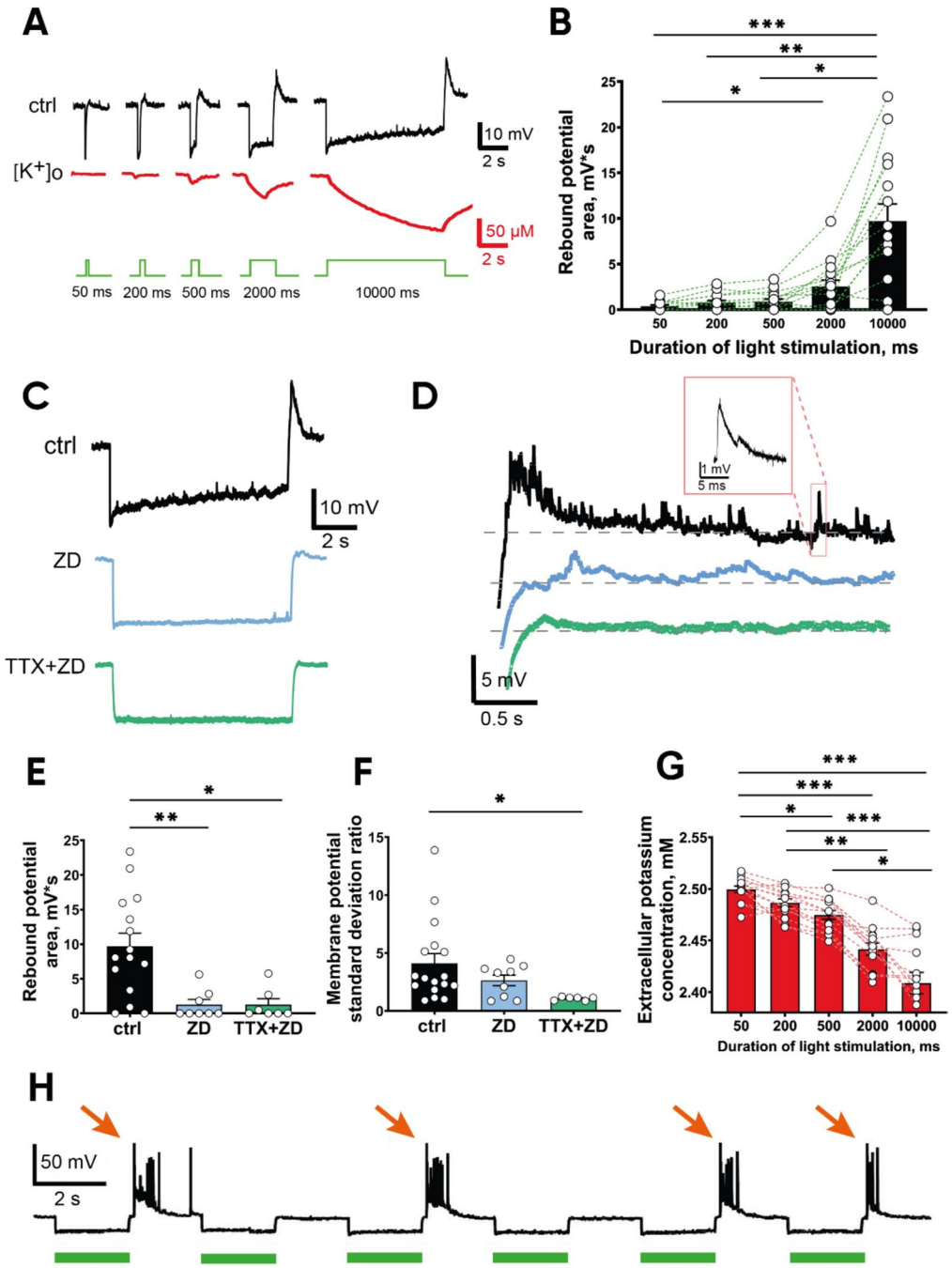

Fig. 3 KR2 photostimulation-mediated hyperpolarization causes the rebound potential. **A** Representative examples of the membrane potential and extracellular potassium ion concentration responses to KR2 photostimulation of different durations. Note a rebound potential at the time the photostimulation was turned off. **B** The dependence of the rebound amplitude on the duration of photostimulation in control conditions ($n=15$, $\chi^2_4=37$, $p<0.001$; Friedman RM analysis, Dunn's post hoc). **C** The membrane potential responses to photostimulation in the control conditions (ctrl), in the presence of the HCN channel blocker ZD7288, 25 µM (ZD), and in the presence of ZD7288 and TTX, 0.5 µM (TTX + ZD). **D** Expanded fragments from C with the rebound depolarizations. A spontaneous response is highlighted in a black frame. Note that the rebound depolarization is blocked by ZD7288, while the spontaneous activity is abolished in the presence of TTX. **E** The area of the rebound potential after 10 s photostimulation in control conditions ($n=15$) and in the presence of ZD7288 ($n=8$) and TTX + ZD7288 ($n=7$) ($H_2=12.9$, $p=0.002$; Kruskal–Wallis one-way analysis, Dunn's post hoc). **F** The ratios of the standard deviations of the membrane voltage potentials for the three groups ($H_2=7.6$, $p=0.022$; Kruskal–Wallis one-way analysis, Dunn's post hoc). **G** Reduction of the extracellular potassium concentration in response to photostimulation of different durations ($n=14$, $\chi^2_4=54$, $p<0.001$; Friedman RM analysis, Dunn's post hoc). *$p<0.05$, **$p<0.01$, ***$p<0.001$. **H** A representative recording of the membrane voltage during the perfusion of the slice with the proepileptic solution. Note that the bursts of neuronal firing appear at the time the photostimulation is turned off

HCN channels are known to mediate rebound depolarization [32]. Therefore, we tested whether these channels are involved by applying their antagonist (ZD7288, 25 μM). Application of ZD7288 almost completely abolished the rebound depolarization after 10 s of photostimulation (Fig. 3C–E).

In response to turning off the light stimulation, we observed a transient increase in network activity, manifested by an increased magnitude of membrane voltage fluctuations (Fig. 3D, black trace). To investigate whether this increase in network activity was mediated by HCN channel activity or by the transient neuronal silencing caused by KR2 activation, we measured the standard deviation of the membrane potential before and after light stimulation and calculated the noise ratio as described in the "Methods" section (Fig. 3F). Under control conditions, the noise ratio was greater than 1 in most of the recordings. Application of ZD7288 did not affect the median value of the noise ratio, whereas co-application of ZD7288 and the voltage-gated sodium channel blocker tetrodotoxin (TTX) significantly reduced the noise ratio due to inhibition of network activity in the brain slice (Fig. 3F). The results obtained suggest that silencing of the network by the KR2 photocurrent is followed by a transient increase in network activity, which contributes to the observed rebound depolarization.

Because KR2 pumps sodium ions out of the cell, its activity could cause a decrease in the intracellular concentration of sodium ions, leading to inhibition of Na–K ATPase activity [33]. Such a decrease could lead to a transient increase in the extracellular K^+ concentration during photostimulation, which could also explain the rebound depolarization. We examined this hypothesis by measuring the extracellular potassium ion concentration using an ion-selective electrode in conjunction with patch-clamp recording (Fig. 3A, red line). Our results revealed a minor decline in the extracellular potassium concentration during the photostimulation period (Fig. 3G). Also, no transient increase in extracellular K^+ concentration was observed during and after photostimulation. Because small changes of the extracellular potassium concentration can be attributed to the decrease in driving force for these ions, we concluded that the KR2 photocurrent does not affect the activity of the Na–K ATPase in our preparation.

The above-mentioned observations indicate that the rebound depolarization in response to KR2 photostimulation is predominantly mediated by HCN channel activity and to a lesser extent by a short-term increase in spontaneous network activity. Therefore, we next investigated whether this rebound depolarization can lead to epileptic events. We applied 2 s photostimulation at 0.25 Hz while the slice was perfused with 4-AP-containing proepileptic solution and recorded the membrane voltage of entorhinal neurons (Fig. 3H). Short (0.5–1 s) epileptiform bursts that occur at turning off light stimulation were observed in 5 out of 5 recorded neurons (Fig. 3F). The short discharges observed in our current preparation were comparable to those induced by ChR2 photostimulation described in our previous study [31]. We hypothesized that these HCN channel-mediated rebound bursts of network activity can be used to control spontaneous epileptiform activity.

Optogenetic Control of Epileptiform Activity in Mouse Brain Slice

Next, we attempted to achieve reliable elimination of ictal activity in the slice by applying intermittent photostimulation (Fig. 4). We developed the protocol of KR2 photostimulation, which promotes the elimination of ictal activity in the slice and uses the HCN channel-mediated rebound depolarization to induce firing of principal neurons. To adjust the parameters of KR2 photic stimulation, we used field potential recordings, which allows long-term registrations of epileptiform activity.

Intermittent light stimulation at 0.33 Hz with a stimulus duration of 800 ms reliably interrupted ictal discharges in 5 out of 6 slices (Fig. 4). Each time the light stimulus was turned off, a brief epileptiform discharge occurred in the slices. The ictal activity resumed after the end of photostimulation (Fig. 4).

Next, we investigated what exactly underlies the anti-ictal effect: rhythmic hyperpolarization of neurons or rebound depolarization causing rhythmic activation of the neuronal network. The blocker of HCN channels suppressed the rebound spikes, thus restoring ictal activity (Fig. 4). Thus, the results obtained show that HCN-mediated rebound firing, and not KR2-induced hyperpolarization, is responsible for the disruption of ictal discharge generation in the entorhinal cortex.

Discussion

In the present study, we investigated the effect of KR2 photostimulation on entorhinal cortex neurons in mouse brain slices. To the best of our knowledge, it is the first application of the KR2 sodium pump to influence epileptiform activity. In our 4-AP model of epilepsy, continuous photoactivation of KR2 did not suppress ictal activity; however, using low-frequency regime of stimulation, we were able to replace the ictal discharge generation with the short bursts.

In our experiments, the kinetics and magnitude of photocurrent and its dependence on light intensity were comparable to those observed in other studies [14, 34]. We detected two effects of light stimulation on neuronal populations expressing KR2. The first effect is an acute hyperpolarization induced by an outward sodium photocurrent. Similar

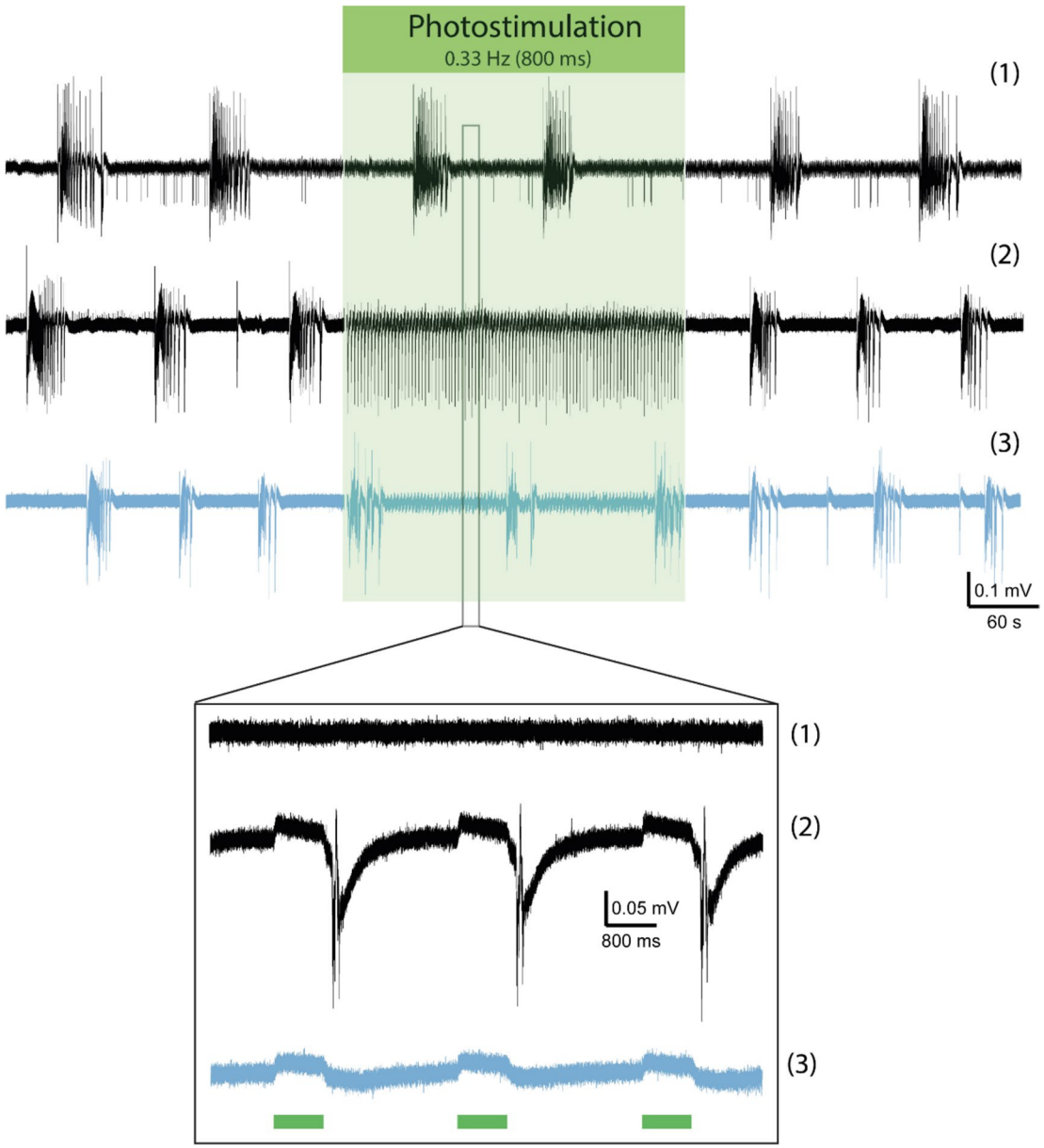

Fig. 4 An example of the epileptiform activity control by KR2 photostimulation. (1) A representative example of ictal activity in the mouse entorhinal cortex. (2) Photostimulation (0.33 Hz, 800 ms stimulus duration) disrupts the generation of ictal discharges. (3) Application of HCN channel blocker ZD7288 restores the ictal activity. The framed inset represents the protocol of KR2 photostimulation (bottom trace) and the extended fragments from the traces above. Note that the short epileptiform bursts emerge at the turning off photostimulation

to KR2, the chloride pump halorhodopsin and the proton pump archaerhodopsin can induce significant hyperpolarization of neurons [4, 31, 35, 36]. However, halorhodopsin activation may lead to an increase in intracellular chloride concentration [37] and consequent enhancement of epileptic activity [38], thus limiting usage of this optogenetic tool for prevention of epilepsy. Changes in cellular pH evoked by archaerhodopsin activation [39, 40] also affect epileptic activity [41]. Thus, KR2 pretends to be a better tool than the previous generation of neuronal silencers because it does not directly affect the neuronal chloride gradient and pumps protons with very low efficiency; instead, it functions primarily as a sodium ion pump under physiological conditions [9, 42]. Therefore, a decrease in the intracellular concentration of sodium ions would be expected upon activation of KR2, leading to a downregulation of the Na–K ATPase activity. However, this effect did not manifest itself in our preparation. We observed only a slight decrease in the extracellular

potassium concentration during KR2 activation, which is contrary to what would be expected in the case of Na–K ATPase downregulation, and which can be attributed to the reduced driving force for the potassium ions during hyperpolarization [43]. Since changes in potassium and chloride ion concentrations can trigger epileptic activity [44], the absence of significant changes in ion concentrations during KR2 activation is an important advantage when using KR2.

The second observed effect of KR2 activation on the membrane voltage was the rebound depolarization leading to the occurrence of discharges each time the stimulation ends. This rebound depolarization is mostly mediated by HCN channels and is comparable to that previously described in the entorhinal cortex [45, 46]. The rebound potential was completely abolished by co-application of the blockers of HCN and voltage-gated sodium channels, indicating that it is not mediated by the persistent changes in ionic gradients, induced by KR2 activation. Thus, we underline that in our preparation, all ionic gradients potentially perturbed by KR2 activation rapidly recover, which may be considered as an additional advantage of using KR2 as a neuronal silencer.

Prevention of epileptic activity by selective optogenetic stimulation of specific cell types in the epileptogenic foci is considered to be a promising approach for the treatment of pharmacoresistant forms of epilepsy [47]. However, the exact treatment protocols have not yet been established. In our preparation, the prolonged hyperpolarization induced by KR2 photocurrent was unable to prevent the ictal discharges in slices. We hypothesize that the activity of neurons with weak or no KR2 expression (presumably, from the medial cortical areas that did not express KR2 in our preparation) may induce ictal-like activity that spreads to the lateral entorhinal cortex despite its continuous photostimulation. We have previously reported that ictal-like events can originate in either medial or lateral cortical regions in the slice and propagate from one cortical region to another, suggesting that even just a fraction of neurons is able to sustain ictal activity [48]. Another potential reason for the inability to prevent the ictal discharges in the brain slice is the non-specific expression of KR2 in all neuronal types. Selective inhibition of glutamatergic neurons is predicted to be significantly more effective [35, 49]. However, targeted inhibition of GABAergic neurons within an appropriate time frame may also be an effective approach [50].

Previously published results suggest that the effect of optogenetic intervention on epileptiform activity may vary depending on experimental preparations. Activation of halorhodopsin in the principal neurons of the hippocampus inhibits "stimulation train-induced bursting" [35] and alters, but not abolishes, the dynamics of epileptiform activity in a lithium-pilocarpine model of epilepsy [51]. In an in vivo kainite model, direct inhibition of hippocampal pyramidal neurons expressing halorhodopsin was able to terminate more than half of the seizures [42]. Previous studies have also attempted to inhibit the activity of principal neurons using optogenetic stimulation of parvalbumin (PV) and somatostatin (SOM) interneurons [52, 53]. Channelrhodopsin-2-mediating activation of PV cells reduces seizures in a kainate model of epilepsy in vivo [53]. Similar results were achieved using the light-activated chloride channels expressed in the dentate gyrus in vivo [54]. However, in the CA3 hippocampus, 5 s-photoactivation of GABAergic interneurons in a 4-AP model in vitro induces only a transient pause in burst generation, whereas a longer period of enhanced interneuronal activity cannot further delay the generation of epileptiform bursts [55]. In addition, switching on light stimulation produced a burst-like discharge in this model. In another study, photodepolarization of PV interneurons changed its effect from anti-ictal to proictal within a few seconds [38, 52]. In another preparation, selective activation of entorhinal PV and SOM interneurons not only failed to stop seizure-like events in entorhinal cortex slices, but also directly triggered them [56]. The ambiguity of these results may be caused by changes in the chloride ion gradient during interneuronal firing, which in turn change the role of interneurons. Such transition is unlikely to occur in our preparation, as the sodium pump is expressed in both principal cells and interneurons [57, 58].

Taken together, these findings suggest that the results of optogenetic inhibition of epileptic networks are highly dependent on the model of seizures used and the location and direction of the optogenetic intervention [59]. In the current study, an in vitro 4-AP model was used, in which ictal activity originate in the entorhinal cortex [23]. Effective inhibition of epileptiform activity in the cortex may therefore require a more precise optogenetic intervention that takes into account its laminar organization or its connections with other brain regions.

Suppression of abnormally synchronized activity by low-frequency stimulation is a promising approach to reduce the severity of epilepsy. Since sustained KR2 activation failed to suppress ictal-like activity in our preparation, we attempted to use HCN channel-mediated rebound firing to induce low-frequency excitation of entorhinal cortex neurons. In contrast to continuous stimulation, intermittent stimulation by brief light pulses was able to disrupt ictal-like activity. Several previous studies have already demonstrated the anti-ictal effect of the low-frequency electric [24, 60] or optogenetic activation of the entorhinal neurons in in vitro models [61]. In kindling models of temporal lobe epilepsy, application of 1 Hz LFS to the hippocampus has been shown to prevent seizure development and subsequent epileptization [62–66]. Prolonged LFS induces synaptic depression, which decreases the excitability of pyramidal neurons and associated networks [62, 66]. However, unlike optogenetic stimulation, electrical stimulation has a non-specific effect

on brain tissue, causing a variety of serious side effects [67, 68] and even causing seizures in some patients [69].

Our previous results demonstrate that low-frequency activation of entorhinal principal neurons by ChR2 disrupts the ictal activity in the brain slice, while their low-frequency hyperpolarization by archaerhodopsin is inefficient [31]. Comparable bursts of neuronal firing were also observed in response to archaerhodopsin stimulation switch-off, but only within a narrow time window during the late phase of the seizure-like event. A more pronounced effect of intermittent hyperpolarization in the present study may be attributed to a greater activation of HCN channels by the stronger photocurrents and longer light pulses.

The implemented KR2 photostimulation protocol, which utilizes the HCN channel-mediated rebound firing, could be an alternative to direct optogenetic activation of these neurons or non-selective electrical stimulation. The implemented approach combines the transient silencing of neuronal activity with the phase-resetting effect of periodic stimulation. We have previously hypothesized that intermittent ChR2 photostimulation disrupts ictal-like activity in the entorhinal cortex by upregulating the Na–K ATPase due to the accumulation of sodium ions inside the cell [31]. The Na–K ATPase activation reduces the network activity due to electrogenic effect and promotes the efficient removal of extracellular potassium ions, thus diminishing the positive feedback in ictal discharge generation mechanism, according to our Epileptor-2 model [70]. As shown previously [71], transient activation of HCN channels by hyperpolarization also upregulates Na–K ATPase in neurons due to co-localization of these proteins in a single Na^+ microdomain. In our case, the sodium accumulation and consequent Na–K ATPase activation is caused by the sodium flux through HCN channels as well as by opening of glutamatergic and voltage-gated sodium channels during the short discharges evoked by light. The KR2-driven hyperpolarization results in silencing and thus synchronization of neurons, which are then readily spiking in response to HCN-mediated depolarizing sag potential. We hypothesize that the resulting sodium accumulation and pump activation prevents ictal discharges in our preparation. Thus, the implemented indirect stimulation of pyramidal neurons may be a more efficient way to disrupt the network synchronization process because it promotes Na–K ATPase activity to a greater extent than direct stimulation.

The proposed approach relies heavily on HCN channels to effectively interrupt ictal activity. However, it may be somewhat problematic in chronic epilepsy, as many reports indicate that HCN channel expression can be downregulated [72–74]. It is also unclear whether the rearranged network in the epileptic brain [23] allows the implemented approach to be effective. Further studies using chronic epilepsy models are needed to address these potential issues.

We conclude that low-frequency photostimulation of the KR2 sodium pump may be an effective protocol for reducing seizure severity. This approach may be effective not only in controlling epileptic activity, but also in other cases associated with spreading depolarizations in the brain such as stroke [75], migraine [76], and traumatic brain injury [77].

Acknowledgements We would like to acknowledge Dr. Elena Y. Proskurina for help in organizing the optogenetic experiment and preliminary results and Mrs. Elizaveta Podoliak for help in production and purification of AAVs.

Author Contribution Conceptualization: AMT, DVA, AVC, and AVZ; funding acquisition: DVA; investigation: AMT, DVA, TYP, VT, AA, EP, VIG, AVC, and AVZ; methodology: AMT, DVA, TYP, and AA; project administration: AVZ; validation: DVA; writing—original draft: AMT, DVA, TYP, VT, AA, EP, VIG, AVC, and AVZ; reviewing and editing: DVA, AVC, and AVZ. All authors have read and agreed to the published version of the manuscript.

Funding This work was supported by Grant No. 21–15-00416 of the Russian Science Foundation.

Data Availability The datasets generated during and/or analyzed during the current study are available from the corresponding author on reasonable request.

Declarations

Ethics Approval All procedures involving animals were followed the European Community Council Directive 86/609/EEC and were approved by the Animal Care and Use Committee of the Sechenov Institute of Evolutionary Physiology and Biochemistry of the Russian Academy of Sciences (Protocol № 1–7 / 2022 of the meeting № 1 of January 27, 2022).

Consent to Participate Not applicable.

Consent for Publication Not applicable.

Conflict of Interest The authors declare no competing interests.

References

1. Sheng J, Liu S, Qin H et al (2018) Drug-resistant epilepsy and surgery. Curr NeuroPharmacol 16. https://doi.org/10.2174/1570159X15666170504123316
2. Cui W, Zack MM, Kobau R, Helmers SL (2015) Health behaviors among people with epilepsy—results from the 2010 National Health Interview Survey. Epilepsy Behav 44:121–126. https://doi.org/10.1016/J.YEBEH.2015.01.011
3. Massey S, Banwell B (2018) Clinical implications of status epilepticus in children. Lancet Child Adolesc Health 2:81. https://doi.org/10.1016/S2352-4642(17)30175-X
4. Chow BY, Han X, Dobry AS et al (2010) High-performance genetically targetable optical neural silencing by light-driven proton pumps. Nature 463(7277):98–102. https://doi.org/10.1038/nature08652
5. Fenno L, Yizhar O, Deisseroth K (2011) The development and application of optogenetics. Annu Rev Neurosci 34:389–412. https://doi.org/10.1146/ANNUREV-NEURO-061010-113817

6. Tye KM, Deisseroth K (2012) Optogenetic investigation of neural circuits underlying brain disease in animal models. Nat Rev Neurosci 13:251–266. https://doi.org/10.1038/NRN3171
7. Yizhar O, Fenno LE, Davidson TJ et al (2011) Optogenetics in neural systems. Neuron 71:9–34. https://doi.org/10.1016/J.NEURON.2011.06.004
8. Camporeze B, Manica BA, Alves Bonafé G et al (2018) Optogenetics: the new molecular approach to control functions of neural cells in epilepsy, depression and tumors of the central nervous system. Am J Cancer Res 8:1900
9. Inoue K, Ono H, Abe-Yoshizumi R et al (2013) A light-driven sodium ion pump in marine bacteria. Nat Commun 4:1678. https://doi.org/10.1038/ncomms2689
10. Kwon SK, Kim BK, Song JY et al (2013) Genomic makeup of the marine flavobacterium Nonlabens (Donghaeana) dokdonensis and identification of a novel class of rhodopsins. Genome Biol Evol 5:187–199. https://doi.org/10.1093/GBE/EVS134
11. Li H, Sineshchekov OA, Da Silva GFZ, Spudich JL (2015) In vitro demonstration of dual light-driven Na^+/H^+ pumping by a microbial rhodopsin. Biophys J 109:1446–1453. https://doi.org/10.1016/J.BPJ.2015.08.018
12. Balashov SP, Imasheva ES, Dioumaev AK et al (2014) Light-driven Na^+ pump from *Gillisia limnaea*: a high-affinity Na^+ binding site is formed transiently in the photocycle. Biochemistry 53:7549–7561. https://doi.org/10.1021/bi501064n
13. Kato HE, Inoue K, Abe-Yoshizumi R et al (2015) Structural basis for Na(+) transport mechanism by a light-driven Na(+) pump. Nature 521:48–53. https://doi.org/10.1038/NATURE14322
14. Hososhima S, Kandori H, Tsunoda SP (2021) Ion transport activity and optogenetics capability of light-driven Na+-pump KR2. PLoS ONE 16:e0256728. https://doi.org/10.1371/journal.pone.0256728
15. Beppu K, Sasaki T, Tanaka KF et al (2014) Optogenetic countering of glial acidosis suppresses glial glutamate release and ischemic brain damage. Neuron 81:314–320. https://doi.org/10.1016/J.NEURON.2013.11.011
16. Deisseroth K (2011) Optogenetics. Nat Methods 8:26–29. https://doi.org/10.1038/NMETH.F.324
17. Hegemann P, Möglich A (2011) Channelrhodopsin engineering and exploration of new optogenetic tools. Nat Methods 8:39–42. https://doi.org/10.1038/NMETH.F.327
18. Vismer MS, Forcelli PA, Skopin MD et al (2015) The piriform, perirhinal, and entorhinal cortex in seizure generation. Front Neural Circuits 9. https://doi.org/10.3389/FNCIR.2015.00027
19. Kügler S, Kilic E, Bähr M (2003) Human synapsin 1 gene promoter confers highly neuron-specific long-term transgene expression from an adenoviral vector in the adult rat brain depending on the transduced area. Gene Therapy 10(4):337–347. https://doi.org/10.1038/sj.gt.3301905
20. Hedegaard C, Kjaer-Sorensen K, Madsen LB et al (2013) Porcine synapsin 1: *SYN1* gene analysis and functional characterization of the promoter. FEBS Open Bio 3:411–420. https://doi.org/10.1016/j.fob.2013.10.002
21. Challis RC, Ravindra Kumar S, Chan KY et al (2019) Systemic AAV vectors for widespread and targeted gene delivery in rodents. Nat Protoc 14:379–414. https://doi.org/10.1038/S41596-018-0097-3
22. Paxinos G, Watson C, Watson C (2007) The rat brain in stereotaxic coordinates sixth edition, 6TH edn. Elsevier Academic Press, London
23. Avoli M, D'Antuono M, Louvel J et al (2002) Network and pharmacological mechanisms leading to epileptiform synchronization in the limbic system in vitro. Prog Neurobiol 68:167–207. https://doi.org/10.1016/S0301-0082(02)00077-1
24. Barbarosie M, Avoli M (1997) CA3-driven hippocampal-entorhinal loop controls rather than sustains in vitro limbic seizures. J Neurosci 17:9308–9314. https://doi.org/10.1523/JNEUROSCI.17-23-09308.1997
25. Soboleva EB, Amakhin DV, Sinyak DS, Zaitsev AV (2022) Modulation of seizure-like events by the small conductance and ATP-sensitive potassium ion channels. Biochem Biophys Res Commun 623:74–80. https://doi.org/10.1016/j.bbrc.2022.07.057
26. Amakhin DV, Ergina JL, Chizhov AV, Zaitsev AV (2016) Synaptic conductances during interictal discharges in pyramidal neurons of rat entorhinal cortex. Front Cell Neurosci 10. https://doi.org/10.3389/fncel.2016.00233
27. Amakhin DV, Soboleva EB, Ergina JL et al (2018) Seizure-induced potentiation of AMPA receptor-mediated synaptic transmission in the entorhinal cortex. Front Cell Neurosci 12:486. https://doi.org/10.3389/fncel.2018.00486
28. Huberfeld G, Blauwblomme T, Miles R (2015) Hippocampus and epilepsy: findings from human tissues. Rev Neurol (Paris) 171:236–251. https://doi.org/10.1016/J.NEUROL.2015.01.563
29. Lévesque M, Biagini G, de Curtis M et al (2021) The pilocarpine model of mesial temporal lobe epilepsy: over one decade later, with more rodent species and new investigative approaches. Neurosci Biobehav Rev 130:274–291. https://doi.org/10.1016/J.NEUBIOREV.2021.08.020
30. De Curtis M, Avoli M (2016) GABAergic networks jump-start focal seizures. Epilepsia 57:679. https://doi.org/10.1111/EPI.13370
31. Proskurina EY, Chizhov AV, Zaitsev AV (2022) Optogenetic low-frequency stimulation of principal neurons, but not parvalbumin-positive interneurons, prevents generation of ictal discharges in rodent entorhinal cortex in an in vitro 4-aminopyridine model. Int J Mol Sci 24:195. https://doi.org/10.3390/ijms24010195
32. Wang XX, Jin Y, Sun H et al (2016) Characterization of rebound depolarization in neurons of the rat medial geniculate body in vitro. Neurosci Bull 32:16. https://doi.org/10.1007/S12264-015-0006-5
33. Horisberger JD, Kharoubi-Hess S (2002) Functional differences between α subunit isoforms of the rat Na, K-ATPase expressed in Xenopus oocytes. J Physiol 539:669. https://doi.org/10.1113/JPHYSIOL.2001.013201
34. Hoque MR, Ishizuka T, Inoue K et al (2016) A chimera Na+-pump rhodopsin as an effective optogenetic silencer. PLoS One 11. https://doi.org/10.1371/JOURNAL.PONE.0166820
35. Tønnesen J, Sørensen AT, Deisseroth K et al (2009) Optogenetic control of epileptiform activity. Proc Natl Acad Sci U S A 106:12162. https://doi.org/10.1073/PNAS.0901915106
36. Hedrick T, Danskin B, Larsen RS et al (2016) Characterization of channelrhodopsin and archaerhodopsin in cholinergic neurons of Cre-Lox transgenic mice. PLoS One 11:e0156596. https://doi.org/10.1371/JOURNAL.PONE.0156596
37. Alfonsa H, Merricks EM, Codadu NK et al (2015) The contribution of raised intraneuronal chloride to epileptic network activity. J Neurosci 35:7715–7726. https://doi.org/10.1523/JNEUROSCI.4105-14.2015
38. Burman RJ, Selfe JS, Lee JH et al (2019) Excitatory GABAergic signalling is associated with benzodiazepine resistance in status epilepticus. Brain 142:3482–3501. https://doi.org/10.1093/BRAIN/AWZ283
39. El-Gaby M, Zhang Y, Wolf K et al (2016) Archaerhodopsin selectively and reversibly silences synaptic transmission through altered pH. Cell Rep 16:2259. https://doi.org/10.1016/J.CELREP.2016.07.057
40. Donahue CET, Siroky MD, White KA (2021) An optogenetic tool to raise intracellular pH in single cells and drive localized membrane dynamics. J Am Chem Soc 143:18877–18887. https://doi.org/10.1021/jacs.1c02156
41. Xiong ZQ, Saggau P, Stringer JL (2000) Activity-dependent intracellular acidification correlates with the duration of seizure

activity. J Neurosci 20:1290–1296. https://doi.org/10.1523/JNEUROSCI.20-04-01290.2000
42. Kovalev K, Astashkin R, Gushchin I et al (2020) Molecular mechanism of light-driven sodium pumping. Nat Commun 11. https://doi.org/10.1038/S41467-020-16032-Y
43. Contreras SA, Schleimer JH, Gulledge AT, Schreiber S (2021) Activity-mediated accumulation of potassium induces a switch in firing pattern and neuronal excitability type. PLoS Comput Biol 17:e1008510. https://doi.org/10.1371/JOURNAL.PCBI.1008510
44. Proskurina EYu, Zaitsev AV (2022) Regulation of potassium and chloride concentrations in nervous tissue as a method of anticonvulsant therapy. J Evol Biochem Physiol 58:1275–1292. https://doi.org/10.1134/S0022093022050015
45. Shah NM, Pisapia DJ, Maniatis S et al (2004) Visualizing sexual dimorphism in the brain. Neuron 43:313–319. https://doi.org/10.1016/j.neuron.2004.07.008
46. Albertson AJ, Yang J, Hablitz JJ (2011) Decreased hyperpolarization-activated currents in layer 5 pyramidal neurons enhances excitability in focal cortical dysplasia. J Neurophysiol 106:2189–2200. https://doi.org/10.1152/JN.00164.2011
47. Bui A, Kim HK, Maroso M, Soltesz I (2015) Microcircuits in epilepsy: heterogeneity and hub cells in network synchronization. Cold Spring Harb Perspect Med 5. https://doi.org/10.1101/CSHPERSPECT.A022855
48. Chizhov AV, Amakhin DV, Smirnova EY, Zaitsev AV (2022) Ictal wavefront propagation in slices and simulations with conductance-based refractory density model. PLoS Comput Biol 18. https://doi.org/10.1371/JOURNAL.PCBI.1009782
49. Krook-Magnuson E, Armstrong C, Oijala M, Soltesz I (2013) On-demand optogenetic control of spontaneous seizures in temporal lobe epilepsy. Nat Commun 4(1):1–8. https://doi.org/10.1038/ncomms2376
50. Călin A, Ilie AS, Akerman CJ (2021) Disrupting epileptiform activity by preventing parvalbumin interneuron depolarization block. J Neurosci 41:9452–9465. https://doi.org/10.1523/JNEUROSCI.1002-20.2021
51. Sukhotinsky I, Chan AM, Ahmed OJ et al (2013) Optogenetic delay of status epilepticus onset in an in vivo rodent epilepsy model. PLoS One 8:e62013. https://doi.org/10.1371/JOURNAL.PONE.0062013
52. Magloire V, Cornford J, Lieb A et al (2019) KCC2 overexpression prevents the paradoxical seizure-promoting action of somatic inhibition. Nat Commun 10(1):1–13. https://doi.org/10.1038/s41467-019-08933-4
53. Krook-Magnuson E, Armstrong C, Oijala M, Soltesz I (2013) On-demand optogenetic control of spontaneous seizures in temporal lobe epilepsy. Nat Commun 4:1376. https://doi.org/10.1038/ncomms2376
54. Acharya AR, Larsen LE, Delbeke J et al (2023) In vivo inhibition of epileptiform afterdischarges in rat hippocampus by light-activated chloride channel, stGtACR2. CNS Neurosci Ther 29:907–916. https://doi.org/10.1111/CNS.14029
55. Ledri M, Madsen MG, Nikitidou L et al (2014) Global optogenetic activation of inhibitory interneurons during epileptiform activity. J Neurosci 34:3364–3377. https://doi.org/10.1523/JNEUROSCI.2734-13.2014
56. Yekhlef L, Breschi GL, Lagostena L et al (2015) Selective activation of parvalbumin- or somatostatin-expressing interneurons triggers epileptic seizurelike activity in mouse medial entorhinal cortex. J Neurophysiol 113:1616–1630. https://doi.org/10.1152/JN.00841.2014
57. Kügler S, Kilic E, Bähr M (2003) Human synapsin 1 gene promoter confers highly neuron-specific long-term transgene expression from an adenoviral vector in the adult rat brain depending on the transduced area. Gene Ther 10:337–347. https://doi.org/10.1038/SJ.GT.3301905
58. Nieuwenhuis B, Haenzi B, Hilton S et al (2020) Optimization of adeno-associated viral vector-mediated transduction of the corticospinal tract: comparison of four promoters. Gene Therapy 28(1):56–74. https://doi.org/10.1038/s41434-020-0169-1
59. Krook-Magnuson E, Szabo GG, Armstrong C et al (2014) Cerebellar directed optogenetic intervention inhibits spontaneous hippocampal seizures in a mouse model of temporal lobe epilepsy. eNeuro 1. https://doi.org/10.1523/ENEURO.0005-14.2014
60. Kano T, Inaba Y, D'Antuono M et al (2015) Blockade of in vitro ictogenesis by low-frequency stimulation coincides with increased epileptiform response latency. J Neurophysiol 114:21–28. https://doi.org/10.1152/JN.00248.2015
61. Shiri Z, Lévesque M, Etter G et al (2017) Optogenetic low-frequency stimulation of specific neuronal populations abates ictogenesis. J Neurosci 37:2999. https://doi.org/10.1523/JNEUROSCI.2244-16.2017
62. Paschen E, Elgueta C, Heining K et al (2020) Hippocampal low-frequency stimulation prevents seizure generation in a mouse model of mesial temporal lobe epilepsy. Elife 9:1–57. https://doi.org/10.7554/ELIFE.54518
63. Ghotbedin Z, Janahmadi M, Mirnajafi-Zadeh J et al (2013) Electrical low frequency stimulation of the kindling site preserves the electrophysiological properties of the rat hippocampal CA1 pyramidal neurons from the destructive effects of amygdala kindling: the basis for a possible promising epilepsy therapy. Brain Stimul 6:515–523. https://doi.org/10.1016/J.BRS.2012.11.001
64. Jalilifar M, Yadollahpour A, Moazedi AA, Ghotbeddin Z (2018) Quantitative analysis of the antiepileptogenic effects of low frequency stimulation applied prior or after kindling stimulation in rats. Front Physiol 9:711. https://doi.org/10.3389/FPHYS.2018.00711/BIBTEX
65. Ghasemi Z, Naderi N, Shojaei A et al (2018) Low frequency electrical stimulation attenuated the epileptiform activity-induced changes in action potential features in hippocampal CA1 pyramidal neurons. Cell J 20:355–360. https://doi.org/10.22074/CELLJ.2018.5443
66. Ghasemi Z, Naderi N, Shojaei A et al (2019) The inhibitory effect of different patterns of low frequency stimulation on neuronal firing following epileptiform activity in rat hippocampal slices. Brain Res 1706:184–195. https://doi.org/10.1016/J.BRAINRES.2018.11.012
67. Fisher R, Salanova V, Witt T et al (2010) Electrical stimulation of the anterior nucleus of thalamus for treatment of refractory epilepsy. Epilepsia 51:899–908. https://doi.org/10.1111/J.1528-1167.2010.02536.X
68. Starnes K, Brinkmann BH, Burkholder D et al (2019) Two cases of beneficial side effects from chronic electrical stimulation for treatment of focal epilepsy. Brain Stimul 12:1077–1079. https://doi.org/10.1016/j.brs.2019.03.077
69. Ochoa-Urrea M, Dayyani M, Sadeghirad B et al (2021) Electrical stimulation-induced seizures and breathing dysfunction: a systematic review of new insights into the epileptogenic and symptomatogenic zones. Front Hum Neurosci 14:612. https://doi.org/10.3389/fnhum.2020.617061
70. Chizhov AV, Zefirov AV, Amakhin DV et al (2018) Minimal model of interictal and ictal discharges "Epileptor-2". PLoS Comput Biol 14:e1006186. https://doi.org/10.1371/JOURNAL.PCBI.1006186
71. Kang Y, Notomi T, Saito M et al (2004) Bidirectional interactions between H-channels and Na+–K+ pumps in mesencephalic trigeminal neurons. J Neurosci 24:3694. https://doi.org/10.1523/JNEUROSCI.5641-03.2004

72. Lin W, Qin J, Ni G et al (2020) Downregulation of hyperpolarization-activated cyclic nucleotide-gated channels (HCN) in the hippocampus of patients with medial temporal lobe epilepsy and hippocampal sclerosis (MTLE-HS). Hippocampus 30:1112–1126. https://doi.org/10.1002/HIPO.23219
73. Powell KL, Ng C, O'Brien T et al (2008) Decreases in HCN mRNA expression in the hippocampus after kindling and status epilepticus in adult rats. Epilepsia 49:1686–1695. https://doi.org/10.1111/J.1528-1167.2008.01593.X
74. Oh YJ, Na J, Jeong JH et al (2012) Alterations in hyperpolarization-activated cyclic nucleotidegated cation channel (HCN) expression in the hippocampus following pilocarpine-induced status epilepticus. BMB Rep 45:635–640. https://doi.org/10.5483/BMBREP.2012.45.11.091
75. Paul S, Candelario-Jalil E (2021) Emerging neuroprotective strategies for the treatment of ischemic stroke: an overview of clinical and preclinical studies. Exp Neurol 335. https://doi.org/10.1016/J.EXPNEUROL.2020.113518
76. Dodick DW (2018) A phase-by-phase review of migraine pathophysiology. Headache 58(Suppl 1):4–16. https://doi.org/10.1111/HEAD.13300
77. Hartings JA, Dreier JP, Ngwenya LB et al (2023) Improving neurotrauma by depolarization inhibition with combination therapy: a phase 2 randomized feasibility trial. Neurosurgery 93:924–931. https://doi.org/10.1227/NEU.0000000000002509